Latin American Journal of Solids and Structures
www.lajss.org

A Parametric Study on the Centrifugal Force-Induced Stress and Displacements in Power-Law Graded Hyperbolic Discs

Abstract

An extensive parametric study on the variation of the centrifugal-force-induced stress and displacements with the inhomogeneity indexes, profile parameters and boundary conditions is conducted based on the author's recently published analytical formulas for radially functionally power-law graded rotating hyperbolic discs under axisymmetric conditions. The radial variation of the thickness of the disc is chosen to obey a hyperbolic function defined either convergent or divergent. In the present work, contrary to the published one, it is assumed that both Young's modulus and density radially vary with the same inhomogeneity index to enable to conduct a parametric study. Under this additional assumption, for the values of the chosen power-law indexes $\beta = -5, 0, 5$ for the material grading rule, and the chosen profile parameters $m = -1,\ -0.75,\ -0.5,\ -0.25, 0,\ 0.25,\ 0.5,\ 0.75,\ 1$ for a hyperbolic disc; the variations of the radial stress, the hoop stress and the radial displacement are all illustrated graphically for a rotating disc whose both surfaces are stress-free, for a rotating disc mounted a rigid shaft at its center and its outer surface is stress-free, and finally for a rotating disc attached a rigid shaft at its center and guided at its outer surface (a rigid casing exists at the outer surface).

Keywords

Elasticity solution, rotating disc, functionally graded, axisymmetric, variable thickness disk.

Vebil Yıldırım[a]*

[a] University of Çukurova, Department of Mechanical Engineering, Adana, TURKEY.
Email: vebil@cu.edu.tr

*Corresponding author

http://dx.doi.org/10.1590/1679-78254229

Received: July 09, 2017
In Revised Form: 7October 07, 2017
Accepted: October 11, 2017
Available online: February 05, 2018

1 INTRODUCTION

Analytical and numerical studies on functionally graded discs have gained a momentum since 1990s. There are numerous studies on stationary/rotating discs with constant/variable thickness and made of an isotropic and homogeneous/non-homogeneous material in the available literature. Some of those studies performed analytically and almost directly relevant to this study are cited in the present paper. In the literature, especially analytical studies on such structures subjected to only the inner pressure are relatively large. In this section, especially, just discs rotating at a constant speed and mainly analytical studies about those are cited.

Güven (1995) studied Tresca's yield condition and the linear hardening rotating solid disk of variable thickness. Eraslan (2003a) obtained analytical solutions for the stress distribution in rotating parabolic solid disks made of an isotropic and homogeneous material based on Tresca's yield criterion associated with the flow rule and linear strain hardening. Eraslan (2003a) showed that the deformation behavior of the convex parabolic disk is similar to that of the uniform thickness disk, but in the case of concave parabolic solid disk, it is different. Eraslan (2003a) also showed mathematically that in the limiting case the parabolic disk solution reduces to the solution of rotating uniform thickness solid disk. Based on Tresca's yield criterion, its associated flow rule and linear strain hardening material behavior, Eraslan (2003b) offered analytical solutions for the elastic–plastic stress distribution in rotating parabolic disks with free, pressurized and radially constrained boundary conditions. In this study it was also shown mathematically that in the limiting case the parabolic disk solution reduces to the uniform disk solution. Apatay and Eraslan (2003) achieved analytical solutions in terms of hypergeometric functions for the elastic deformation of rotating parabolic discs made of isotropic and homogeneous materials. Calderale et al. (2012) studied theoretically a thermoelastic analysis of the Stodola's hyperbolic disk made of an isotropic and homogeneous material, axisymmetric and symmetric with respect to the mid-plane, and subjected to a radially polynomially varying thermal load. Vivio et al. (2014) introduced a theoretical method for the evaluation of elastic stresses and strains in rotating

hyperbolic disks made of an isotropic and homogeneous material. For rotating discs made of an isotropic and homogeneous material, Eraslan and Ciftci (2015) used a disk profile changing with an exponential function. Yıldırım (2017) offered all-in-one formulas for uniform discs, cylinders and spheres subjected to the mechanical and thermal loads. In this Reference centrifugal force-induced, heat-induced, and pressure-induced elastic responses have all been considered for those structures made of an isotropic and homogeneous material.

As to rotating discs made of functionally graded materials, material grading function was chosen as a simple power function in some References (Horgan and Chan, 1999a,b, You et al. (2007); Bayat et al., 2008; Çallıoğlu et al., 2011; Yıldırım, 2016; Gang, 2017), and as an exponential function in some studies (Zenkour, 2005, 2007; Zenkour and Mashat, 2011; Eraslan and Arslan, 2015) to get analytical solutions. From those, Horgan and Chan (1999a,b) gave explicit solutions for rotating discs of constant density and thickness. Zenkour (2005) studied analytically exponentially graded rotating annular discs with constant thickness. Eraslan and Akış (2006) used two variants of a parabolic function for disks made of functionally graded materials. Zenkour (2007) extended his study (Zenkour, 2005) for such discs with rigid casing. Bayat et al. (2008), based on the power-law distribution, gave both analytical and semi-analytical elastic solutions for axisymmetric rotating hollow discs with parabolic and hyperbolic thickness profiles. This semi-analytic solution was obtained by dividing the disc with varying thickness into sub-domains with uniform thickness. By taking Young's modulus, thermal expansion coefficient and density to be functions of the radial coordinate, a closed form solution of rotating uniform circular disks made of power-law graded materials subjected to a constant angular velocity and a uniform temperature is proposed by You et al. (2007). Vivio and Vullo (2007) presented an analytical procedure based on the hypergeometric differential equation for evaluation of elastic stresses and strains in rotating solid or annular conical disks subjected to thermal load, and having a fictitious density variation along the radius. Vivio and Vullo (2007) also verified their analytical results with finite element solutions. Vullo and Vivio (2008) presented an analytical procedure for evaluation of elastic stresses and strains in non-linear variable thickness rotating disks, either solid or annular, subjected to thermal load, and having a fictitious density variation along the radius. Thickness variation of disks was described by means of a power of linear function by Vullo and Vivio (2008). Peng and Li (2009) studied a thermoelastic problem of a circular annulus made of functionally graded materials with an arbitrary gradient. Peng, and Li (2012) also studied effects of gradient on stress distribution in rotating functionally graded solid disks. Zenkour and Mashat (2011) used the modified Runga-Kutte algorithm in their numerical analysis. Çallıoğlu et al. (2011) performed an exact stress analysis of annular rotating discs made of functionally graded materials by assuming that both elasticity modulus and material density vary radially as a function of a simple power rule with the same inhomogeneity parameter. Hassani et al. (2011) obtained distributions of stress and strain components of rotating hyperbolic disks with non-uniform material properties subjected to a power form thermo-elastic loading under different boundary conditions by semi-exact methods of Liao's homotopy analysis method. Argeso (2012) presented analytical solutions for two different annular rotating disk problems for the elastic stress state: The first problem involves an exponentially variable profile rotating disk made of an isotropic and homogeneous material, the second is a uniform disc made of exponentially functionally graded materials. Nejad et al. (2013, 2014) gave a closed-form analytical solution in terms of hyper geometric functions to elastic analysis of exponentially functionally graded stationary discs subjected to internal and external pressures. Eraslan and Arslan (2015) developed analytical and numerical solutions to a rotating uniform thickness exponentially functionally graded (FGM) solid and annular disks. Yıldırım (2016) studied the exact elastic response of a rotating disk having a continuously varying hyperbolic thickness profile under different boundary conditions. Both convergent-hyperbolic and divergent-hyperbolic disk profiles together with uniform profile are all studied. Power-law grading is used for material gradation pattern. Yıldırım's (2016) formulation comprises both continuously variations of elasticity modulus and material density including continuously variation of the thickness of the disc except variation of Poisson's ratios. Contrary to the literature all effects affecting the elastic behavior of the disk with varying thickness such as internal and external pressures including rotation at a constant angular velocity are all studied under four physical boundary conditions and presented in compact forms in Yıldırım's study (Yıldırım, 2016). Recently, Gang (2017) analytically studied the stress analysis of hyperbolic simple-power law graded rotating discs under stress-free conditions for four convergent disc profiles and negative inhomogeneity indexes.

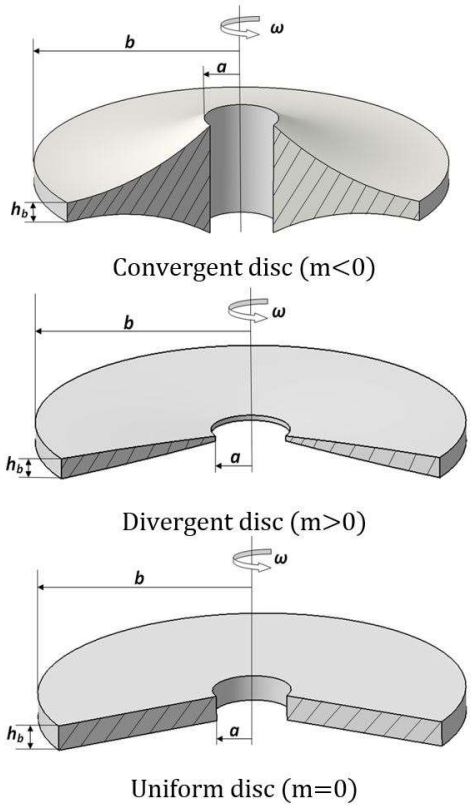

Figure 1: *3-D view of convergent/divergent hyperbolic and uniform disc profiles*

In this study, under the additional assumption that both Young's modulus and material density have a variation with the same inhomogeneity index, closed-form formulas derived by Yıldırım (2016) are employed in the present work in a customized form to study the variation of centrifugal force-induced stress and displacements in power-law graded hyperbolic discs with inhomogeneity parameter, profile parameter and boundary conditions (Fig. 1). As mentioned above, radial variation of Poisson's ratio is neglected. As You et al. (2007) expressed "Doubling Poisson's ratio, the radial and circumferential stresses and radial displacement have very few changes. However, doubling Young's modulus, the radial stress is increased obviously, the circumferential stress is raised greatly, and the radial displacement is reduced noticeably. Therefore, compared to the effects of Young's modulus, the variation of Poisson's ratio can be omitted."

2 EXPANDING YILDIRIM'S (2016) FORMULAS

The disk whose inner radius is denoted by a and outer radius is denoted by b is assumed to be symmetric with respect to the mid plane, and its profile vary radially continuously in an hyperbolical form

$$h(r) = h_a \left(\frac{r}{a} \right)^m \tag{1}$$

where h_a is the thickness of the disc at the inner surface, r is the radial coordinate, and m is the disc profile parameter. In Eq. (1), a uniform disc profile is obtained with m=0, a convergent hyperbolic dick profile is attained with m<0 and for m>0 a divergent hyperbolic disc profile is reached (Fig. 1).

Yıldırım (2016) solved the following nonhomogeneous equation governing the elastostatic behavior of a rotating disc made of functionally graded materials for the hyperbolic discs rotating at a constant angular velocity, ω.

$$\frac{\left(-1+m\nu+\beta\nu\right)}{r^2}u_r + \frac{\left(1+m+\beta\right)}{r}u_r^{'} + u_r^{''} = -\frac{r^{1+q-\beta}\left(1-\nu^2\right)\rho_a\omega^2}{E_a} \tag{2}$$

In the above equation, the prime symbol, (′), denotes the derivative with respect to the radial coordinate. Poisson's ratio is indicated by ν; E_a and ρ_a are the inner surface values of elasticity modulus and the density, respectively. Representing Young's modulus by E, and material density by ρ, in the above either

$$E(r)=E_a\left(\frac{r}{a}\right)^{\beta}$$
$$\rho(r)=\rho_a\left(\frac{r}{a}\right)^{q} \tag{3a}$$

$$E(r)=E_b\left(\frac{r}{b}\right)^{\beta}$$
$$\rho(r)=\rho_b\left(\frac{r}{b}\right)^{q} \tag{3b}$$

may be applied as a material grading rule. In Eq. (3) β and q are called inhomogeneity parameters for both elasticity modulus and density, respectively. If one suppose that *Material-a* is located at the inner surface and *Material-b* is located at the outer surface, inhomogeneity parameters in these equations are defined as follows

$$\beta=\frac{\ln\left(\frac{E_a}{E_b}\right)}{\ln\left(\frac{a}{b}\right)}=\frac{\ln\left(\frac{E_b}{E_a}\right)}{\ln\left(\frac{b}{a}\right)} \tag{4a}$$

$$q=\frac{\mathrm{In}\left(\frac{\rho a}{\rho b}\right)}{\mathrm{In}\left(\frac{a}{b}\right)}=\frac{\mathrm{In}\left(\frac{\rho b}{\rho a}\right)}{\mathrm{In}\left(\frac{b}{a}\right)} \tag{4b}$$

Derivation of Eq. (2) is presented in Appendix A. The general solution of Eq. (2) is written in terms of unknown coefficients C_1 and C_2 as follows (Yıldırım, 2016)

$$u_r=r^{\frac{1}{2}(-m-\beta-\xi)}\left(C_1+C_2r^{\xi}\right)+r^{3+q-\beta}\frac{\left(-1+\nu^2\right)\rho_a\omega^2}{E_a\left(8+q\left(6+q-\beta\right)-3\beta+\beta\nu+m\left(3+q-\beta+\nu\right)\right)} \tag{5}$$

Where

$$\xi=\sqrt{\left(4+\left(m+\beta\right)\left(m+\beta-4\nu\right)\right)} \tag{6}$$

Yıldırım (2016) presented explicit definitions of unknown coefficients, C_1 and C_2, for all possible boundary conditions. Although Yıldırım's (2016) formulas are valid for the different inhomogeneity parameters for both elasticity modulus and material density, in the present study, those indexes are assumed to be equal to each other, that is $q=\beta$ is to be used. That is those formulas will be customized for $q=\beta$ to allow a parametric study.

Let's do this. Under this assumption, $q=\beta$, the solution in Eq. (5) together with Eq. (3a) turns into the following

$$u_r=\frac{r^3\left(-1+\nu^2\right)\rho_a\omega^2}{E_a\left(8+m\left(3+\nu\right)+\beta\left(3+\nu\right)\right)}+r^{\frac{1}{2}(-m-\beta-\xi)}\left(C_1+r^{\xi}C_2\right) \tag{7}$$

Boundary conditions considered in the present study are presented in Fig. 2. For those boundary conditions and $q = \beta$, the closed-form expressions of the radial displacement, radial and hoop stresses are presented in Tables 1-3.

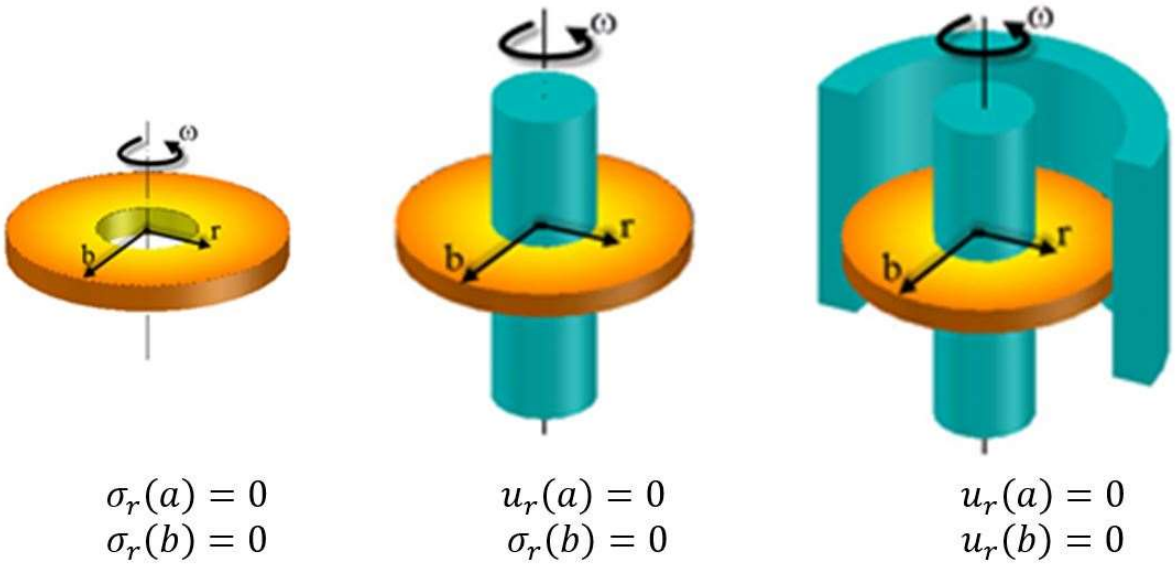

$$\sigma_r(a) = 0 \quad \sigma_r(b) = 0 \qquad u_r(a) = 0 \quad \sigma_r(b) = 0 \qquad u_r(a) = 0 \quad u_r(b) = 0$$

Figure 2: *Boundary conditions considered in the present study*

Table 1: *Closed-form formulas for free-free boundary conditions*

FREE-FREE

$$u_r = \frac{\rho_a \omega^2}{E_a(\beta(\nu+3)+m(\nu+3)+8)}\left(\frac{2(\nu-1)(\nu+1)(\nu+3)a^{\xi/2}b^{\xi/2}r^{\frac{1}{2}(-\beta-m-\xi)}\left(a^{\xi/2}b^{\frac{1}{2}(\beta+m+6)}-b^{\xi/2}a^{\frac{1}{2}(\beta+m+6)}\right)}{(a^\xi-b^\xi)(\beta+m-2\nu+\xi)}\right.$$
$$\left.-\frac{2(\nu-1)(\nu+1)(\nu+3)r^{\frac{1}{2}(-\beta-m+\xi)}\left(a^{\frac{1}{2}(\beta+m+\xi+6)}-b^{\frac{1}{2}(\beta+m+\xi+6)}\right)}{(a^\xi-b^\xi)(-\beta-m+2\nu+\xi)}+(\nu^2-1)r^3\right)$$

$$\sigma_r = \frac{1}{(a^\xi-b^\xi)(\beta(\nu+3)+m(\nu+3)+8)}\left\{(\nu+3)\rho_a\omega^2 a^{-\beta}r^{\frac{1}{2}(\beta-m-\xi-2)}\left(\left(r^\xi-b^\xi\right)a^{\frac{1}{2}(\beta+m+\xi+6)}\right.\right.$$
$$\left.\left.+a^\xi\left(b^{\frac{1}{2}(\beta+m+\xi+6)}-r^{\frac{1}{2}(\beta+m+\xi+6)}\right)-r^\xi b^{\frac{1}{2}(\beta+m+\xi+6)}+b^\xi r^{\frac{1}{2}(\beta+m+\xi+6)}\right)\right\}$$

$$\sigma_\theta = \frac{1}{\left((a^\xi-b^\xi)(\beta(\nu+3)+m(\nu+3)+8)(\beta+m-2\nu-\xi)(\beta+m-2\nu+\xi)\right)}\left(\rho_a\omega^2 a^{-\beta}r^{\frac{1}{2}(\beta-m-\xi-2)}\left((\nu\right.\right.$$
$$+3)a^{\frac{1}{2}(\beta+m+\xi+6)}\left(r^\xi(\nu(\beta+m-\xi)-2)(\beta+m-2\nu+\xi)\right.$$
$$\left.-b^\xi(\beta+m-2\nu-\xi)(\nu(\beta+m+\xi)-2)\right)$$
$$+a^\xi(\beta+m-2\nu-\xi)\left((\nu+3)b^{\frac{1}{2}(\beta+m+\xi+6)}(\nu(\beta+m+\xi)-2)\right.$$
$$\left.-(3\nu+1)(\beta+m-2\nu+\xi)r^{\frac{1}{2}(\beta+m+\xi+6)}\right)$$
$$+b^{\xi/2}r^{\xi/2}(\beta+m-2\nu+\xi)\left((\nu+3)\left(-r^{\xi/2}\right)b^{\frac{1}{2}(\beta+m+6)}(\nu(\beta+m-\xi)-2)\right.$$
$$\left.\left.\left.-(3\nu+1)b^{\xi/2}r^{\frac{1}{2}(\beta+m+6)}(-\beta-m+2\nu+\xi)\right)\right)\right)$$

Table 2: *Closed-form formulas for fixed-guided boundary conditions*

FIXED-GUIDED

$$u_r = -\frac{1}{E_a(a^\xi - b^\xi)(\beta(\nu+3)+m(\nu+3)+8)}\Big\{(\nu^2-1)\rho_a\omega^2 r^{\frac{1}{2}(-\beta-m-\xi)}((r^\xi - b^\xi)a^{\frac{1}{2}(\beta+m+\xi+6)} + a^\xi(b^{\frac{1}{2}(\beta+m+\xi+6)} - r^{\frac{1}{2}(\beta+m+\xi+6)}) - r^\xi b^{\frac{1}{2}(\beta+m+\xi+6)} + b^\xi r^{\frac{1}{2}(\beta+m+\xi+6)}\Big\}$$

$$\sigma_r = \frac{\rho_a\omega^2 a^{-\beta} r^{\frac{1}{2}(\beta-m-\xi-2)}}{2(a^\xi - b^\xi)(\beta(\nu+3)+m(\nu+3)+8)}\Big\{\Big(a^{\frac{1}{2}(\beta+m+\xi+6)}\left(b^\xi(\beta+m-2\nu+\xi)+r^\xi(-\beta-m+2\nu+\xi)\right) + a^\xi\left(-\left(b^{\frac{1}{2}(\beta+m+\xi+6)}(\beta+m-2\nu+\xi)+2(\nu+3)r^{\frac{1}{2}(\beta+m+\xi+6)}\right)\right) + r^\xi b^{\frac{1}{2}(\beta+m+\xi+6)}(\beta+m-2\nu-\xi)+2(\nu+3)b^\xi r^{\frac{1}{2}(\beta+m+\xi+6)}\Big)\Big\}$$

$$\sigma_\theta = \frac{\rho_a\omega^2 a^{-\beta} r^{\frac{1}{2}(\beta-m-\xi-2)}}{2(a^\xi - b^\xi)(\beta(\nu+3)+m(\nu+3)+8)}\Big\{\Big(a^{\frac{1}{2}(\beta+m+\xi+6)}\left(b^\xi(\nu(\beta+m+\xi)-2)+r^\xi(2-\nu(\beta+m-\xi))\right) + a^\xi\left(b^{\frac{1}{2}(\beta+m+\xi+6)}(2-\nu(\beta+m+\xi))-2(3\nu+1)r^{\frac{1}{2}(\beta+m+\xi+6)}\right) + r^\xi b^{\frac{1}{2}(\beta+m+\xi+6)}(\nu(\beta+m-\xi)-2)+2(3\nu+1)b^\xi r^{\frac{1}{2}(\beta+m+\xi+6)}\Big)\Big\}$$

Table 3: *Closed-form formulas for fixed-free boundary conditions*

FIXED-FREE

$$u_r = \frac{1}{\left(E_a(\beta(\nu+3)+m(\nu+3)+8)(a^\xi(\beta+m-2\nu+\xi)+b^\xi(-\beta-m+2\nu+\xi))\right)}\Big\{\Big((\nu^2-1)\rho_a\omega^2 r^{\frac{1}{2}(-\beta-m-\xi)}\left(a^{\frac{1}{2}(\beta+m+\xi+6)}\left(b^\xi(\beta+m-2\nu-\xi)-r^\xi(\beta+m-2\nu+\xi)\right) + a^\xi\left(2(\nu+3)b^{\frac{1}{2}(\beta+m+\xi+6)}+(\beta+m-2\nu+\xi)r^{\frac{1}{2}(\beta+m+\xi+6)}\right)-2(\nu+3)r^\xi b^{\frac{1}{2}(\beta+m+\xi+6)} + b^\xi(-\beta-m+2\nu+\xi)r^{\frac{1}{2}(\beta+m+\xi+6)}\right)\Big)\Big\}$$

$$\sigma_r = \frac{1}{\left(2(\beta(\nu+3)+m(\nu+3)+8)(a^\xi(\beta+m-2\nu+\xi)+b^\xi(-\beta-m+2\nu+\xi))\right)}\Big\{\Big(\rho_a\omega^2 a^{-\beta} r^{\frac{1}{2}(\beta-m-\xi-2)}\left((b^\xi - r^\xi)a^{\frac{1}{2}(\beta+m+\xi+6)}((\beta+m-2\nu)^2-\xi^2) + 2(\nu+3)a^\xi(\beta+m-2\nu+\xi)\left(b^{\frac{1}{2}(\beta+m+\xi+6)}-r^{\frac{1}{2}(\beta+m+\xi+6)}\right) + 2(\nu+3)b^{\xi/2}r^{\xi/2}(-\beta-m+2\nu+\xi)\left(r^{\xi/2}b^{\frac{1}{2}(\beta+m+6)}-b^{\xi/2}r^{\frac{1}{2}(\beta+m+6)}\right)\right)\Big)\Big\}$$

$$\sigma_\theta = \frac{1}{\left(2(\beta(\nu+3)+m(\nu+3)+8)(a^\xi(\beta+m-2\nu+\xi)+b^\xi(-\beta-m+2\nu+\xi))\right)}\Big\{\Big(\rho_a\omega^2 a^{-\beta} r^{\frac{1}{2}(\beta-m-\xi-2)}\left(a^{\frac{1}{2}(\beta+m+\xi+6)}\left(b^\xi(\beta+m-2\nu-\xi)(\nu(\beta+m+\xi)-2) - r^\xi(\nu(\beta+m-\xi)-2)(\beta+m-2\nu+\xi)\right) + 2a^\xi\left((\nu+3)b^{\frac{1}{2}(\beta+m+\xi+6)}(\nu(\beta+m+\xi)-2)-(3\nu+1)(\beta+m-2\nu+\xi)r^{\frac{1}{2}(\beta+m+\xi+6)}\right) - 2(\nu+3)r^\xi b^{\frac{1}{2}(\beta+m+\xi+6)}(\nu(\beta+m-\xi)-2) - 2(3\nu+1)b^\xi(-\beta-m+2\nu+\xi)r^{\frac{1}{2}(\beta+m+\xi+6)}\right)\Big)\Big\}$$

Çallıoğlu et al. (2011) studied the elastic response of power-graded uniform stress-free rotating disks with boundary conditions: $u_r(a)=0$ and $\sigma_r(b)=0$ (Fig. 2). They assumed that both the Young's modulus and the material density change with the same inhomogeneity index, $q=\beta$, in their formulation as in the present work. However, they further assumed that the thickness of the disc remains constant along the radial coordinate, that is

$m=0$. Yıldırım (2016) also showed that her formulas coincides with Çallıoğlu et al.'s (2011) study under those assumptions stated in this paragraph.

3 A NUMERICAL STUDY

The following geometrical properties are used in the parametric study: $a = 0.02\ m; b = 0.1\ m$. Poisson's ratio is assumed to be constant along the radial coordinate as $\nu=0.3$. Dimensionless elastic stress and displacements are defined as

$$\overline{\sigma}_r = \frac{\sigma_r}{\rho_a \omega^2 b^2}\ ; \quad \overline{\sigma}_\theta = \frac{\sigma_\theta}{\rho_a \omega^2 b^2}\ ; \quad \overline{u}_r = \frac{E_a u_r}{\rho_a \omega^2 b^3} \tag{8}$$

For the values of the chosen simple power-law indexes $\beta = -5, 0, 5$ for the material grading rule (Fig. 3), and the chosen profile parameters $m = -1,\ -0.75,\ -0.5,\ -0.25, 0,\ 0.25,\ 0.5,\ 0.75,\ 1$ for a hyperbolic disc; the variations of the radial stress, the hoop stress and the radial displacement are all illustrated graphically for a rotating disc whose both surfaces are stress-free, for a rotating disc mounted a rigid shaft at its center and its outer surface is stress-free, and finally for a rotating disc attached a rigid shaft at its center and guided at its outer surface (a rigid casing exists at the outer surface) in Figs. 3-5. Some numerical results are also presented in Tables 4-6 to serve as a numerical data for investigators.

According to Eq. (3) the positive inhomogeneity indexes suggest that the outer surface and its vicinity is highly stiffer than the middle and the inner surfaces. However, the inner surface is stiffer than the middle and outer surfaces for the negative inhomogeneity indexes. The results obtained from a parametric study of the present work may be outlined concisely as follows (see Figs 3-5):

Convergent hyperbolic dick profiles, $m<0$, offer smaller elastic field than divergent ones for negative inhomogeneity indexes including isotropic and homogeneous materials with $\beta = 0$. However, for the positive inhomogeneity parameters some differences in the behavior may be observed. For instance, while the hoop stresses are smaller for fixed-free and free-free ends of convergent disc profiles, the radial stresses behave contrarily to this for all boundary conditions. Similar to this, for fixed-free and free-free conditions, convergent profiles having positive inhomogeneity parameter present much smaller radial displacement values.

As expected, fixed-guided discs have higher elastic field than fixed-free and free-free boundary conditions.

For fixed-guided disc and positive inhomogeneity index, hoop stresses are in tension-compression. For other boundary conditions they are in tension. However, negative inhomogeneity parameters offer hoop stresses in tension for all boundary conditions and for both convergent and divergent disc profiles.

While positive inhomogeneity indexes present the maximum hoop stress at the outer surface of the disc, their locations are at the inner surface of the disc for negative inhomogeneity indexes.

It may be noted that Gang (2017) analytically studied convergent hyperbolic discs with $m = -1,\ -0.75,\ -0.5,\ -0.25$, and negative inhomogeneity indexes which may be defined approximately as $\beta = -0.00265$ and $q = -0.019$ under stress-free conditions (free-free). He concluded that radial and tangential stresses in convergent FGM hyperbolic disc with negative inhomogeneity indexes is significantly reduced as compared to FGM uniform disc. This comment is in agreement with the first item of the conclusions given above of Figs. 3-5 and obtained from a widespread search.

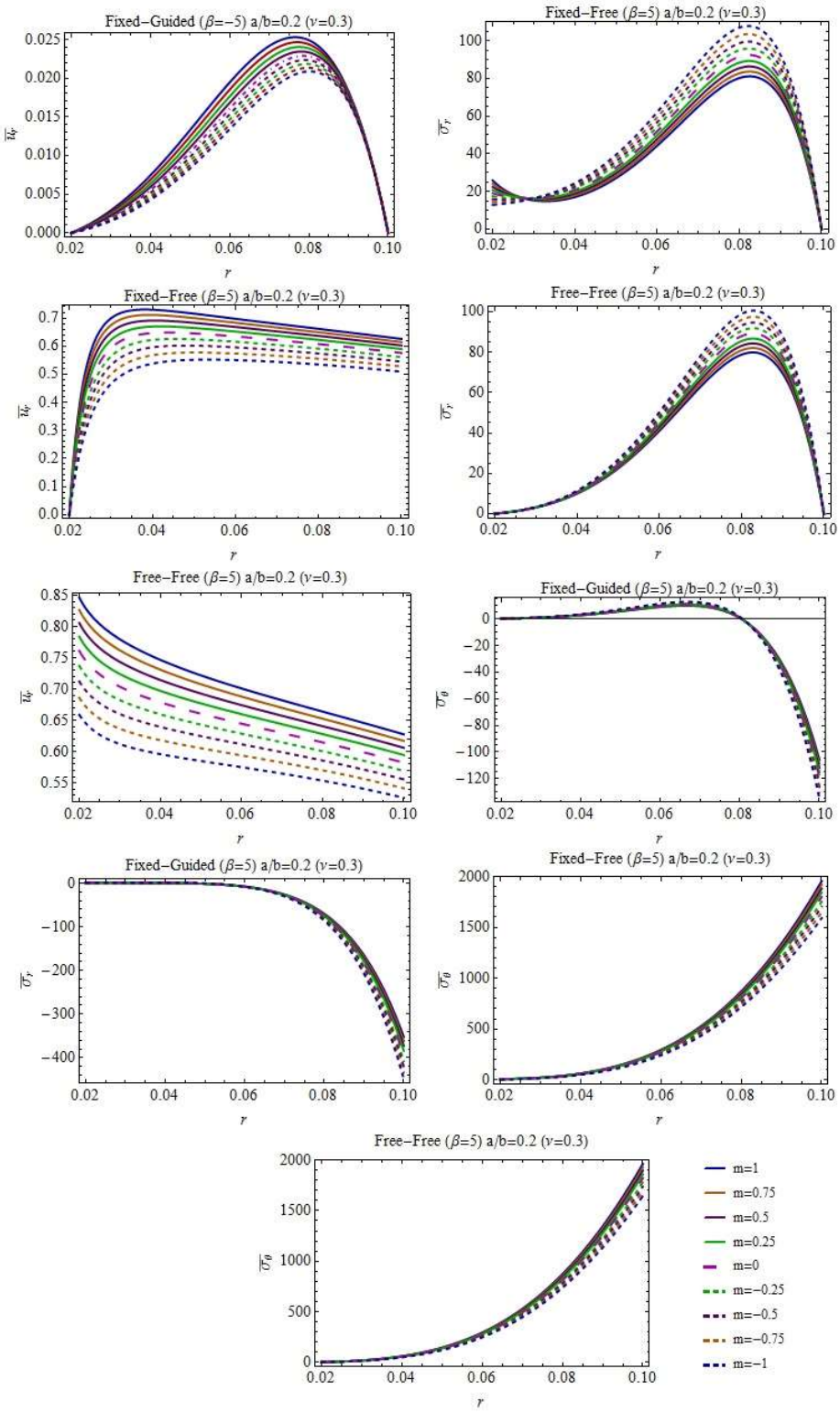

Figure 3: *Variation of the displacement, the radial and hoop stresses with the boundary conditions and profile indexes for* $\beta = 5$

Table 4: *Some numerical results for* $\beta = 5$

r/b	m=1	m=0.75	m=0.5	m=0.25	m=0	m=-0.25	m=-0.50	m=-0.75	m=-1
Dimensionless radial displacement (Free-Free)									
0.2	0.84645	0.82656	0.80574	0.78395	0.76114	0.73728	0.71231	0.68622	0.65899
0.4	0.74676	0.73108	0.71459	0.69725	0.67901	0.65981	0.63963	0.61841	0.59612
0.6	0.70113	0.68815	0.67448	0.66007	0.64487	0.62885	0.61194	0.59411	0.57531
0.8	0.66415	0.65279	0.64082	0.62820	0.61488	0.60082	0.58598	0.57032	0.55379
1.	0.62776	0.61731	0.60631	0.59470	0.58245	0.56953	0.55588	0.54148	0.52627
Dimensionless radial displacement (Fixed-Free)									
0.4	0.72968	0.71097	0.69094	0.66948	0.64649	0.62186	0.59552	0.56741	0.53754
0.6	0.69733	0.68322	0.66811	0.65189	0.63445	0.61567	0.59544	0.57364	0.55023
0.8	0.66155	0.64935	0.63630	0.62231	0.60728	0.59109	0.57365	0.55485	0.53463
1.	0.62540	0.61420	0.60222	0.58937	0.57557	0.56071	0.54469	0.52743	0.50887
Dimensionless radial displacement (Fixed-Fixed)									
0.4	0.03431	0.03496	0.03565	0.03631	0.03697	0.03760	0.03821	0.03878	0.03930
0.6	0.02797	0.02867	0.02939	0.03015	0.03093	0.03173	0.03255	0.03340	0.03426
0.8	0.01698	0.01744	0.01792	0.01842	0.01895	0.01950	0.02008	0.02069	0.02132
Dimensionless radial stress (Free-Free)									
0.4	9.95242	10.1466	10.3411	10.5343	10.7244	10.9092	11.0859	11.2514	11.402
0.6	41.0716	42.0999	43.1677	44.2746	45.4194	46.6	47.8127	49.0521	50.3108
0.8	78.8049	80.9321	83.1634	85.504	87.9584	90.5305	93.2231	96.0375	98.9726
Dimensionless radial stress (Fixed-Free)									
0.2	25.7854	24.0535	22.3476	20.6702	19.024	17.4126	15.8403	14.3124	12.835
0.4	17.0016	17.9167	18.8648	19.835	20.8123	21.7777	22.7078	23.5746	24.3465
0.6	44.2218	45.9081	47.7453	49.7422	51.904	54.23	56.7115	59.3291	62.0503
0.8	80.2097	82.7282	85.4451	88.382	91.5599	94.9984	98.7125	102.71	106.988
Dimensionless radial stress (Fixed-Fixed)									
0.2	1.27037	1.24024	1.2087	1.17568	1.14113	1.10496	1.06714	1.02761	0.98635
0.4	0.26598	0.33666	0.41691	0.50770	0.61004	0.72486	0.85307	0.99540	1.15236
0.6	-7.6694	-7.75575	-7.82984	-7.88779	-7.92493	-7.93568	-7.91341	-7.8504	-7.7377
0.8	-69.936	-71.693	-73.5186	-75.4127	-77.3735	-79.397	-81.4768	-83.6031	-85.7622
1.	-352.50	-362.394	-372.817	-383.808	-395.404	-407.644	-420.567	-434.21	-448.605
Dimensionless hoop stress (Free-Free)									
0.2	4.23223	4.13278	4.0287	3.91975	3.80571	3.68638	3.56156	3.43111	3.29495
0.4	62.7265	61.5302	60.2696	58.9403	57.5379	56.0579	54.496	52.8479	51.1101
0.6	296.279	291.33	286.113	280.609	274.799	268.662	262.179	255.329	248.095
0.8	873.758	859.853	845.199	829.743	813.432	796.211	778.024	758.818	738.543
1.	1961.74	1929.1	1894.7	1858.43	1820.17	1779.77	1737.13	1692.11	1644.6
Dimensionless hoop stress (Fixed-Free)									
0.2	7.73562	7.21605	6.70429	6.20105	5.70719	5.22377	4.75209	4.29372	3.85051
0.4	63.4748	62.2522	60.9344	59.509	57.9629	56.2822	54.4535	52.4649	50.3071
0.6	295.687	290.475	284.906	278.938	272.524	265.616	258.165	250.124	241.456
0.8	870.842	855.985	840.101	823.076	804.784	785.095	763.88	741.019	716.417
1.	1954.38	1919.37	1881.93	1841.79	1798.65	1752.21	1702.16	1648.23	1590.21
Dimensionless hoop stress (Fixed-Fixed)									
0.2	0.381112	0.372071	0.362609	0.352705	0.342338	0.331489	0.320142	0.308283	0.295904
1.	-105.751	-108.718	-111.845	-115.142	-118.621	-122.293	-126.17	-130.263	-134.582

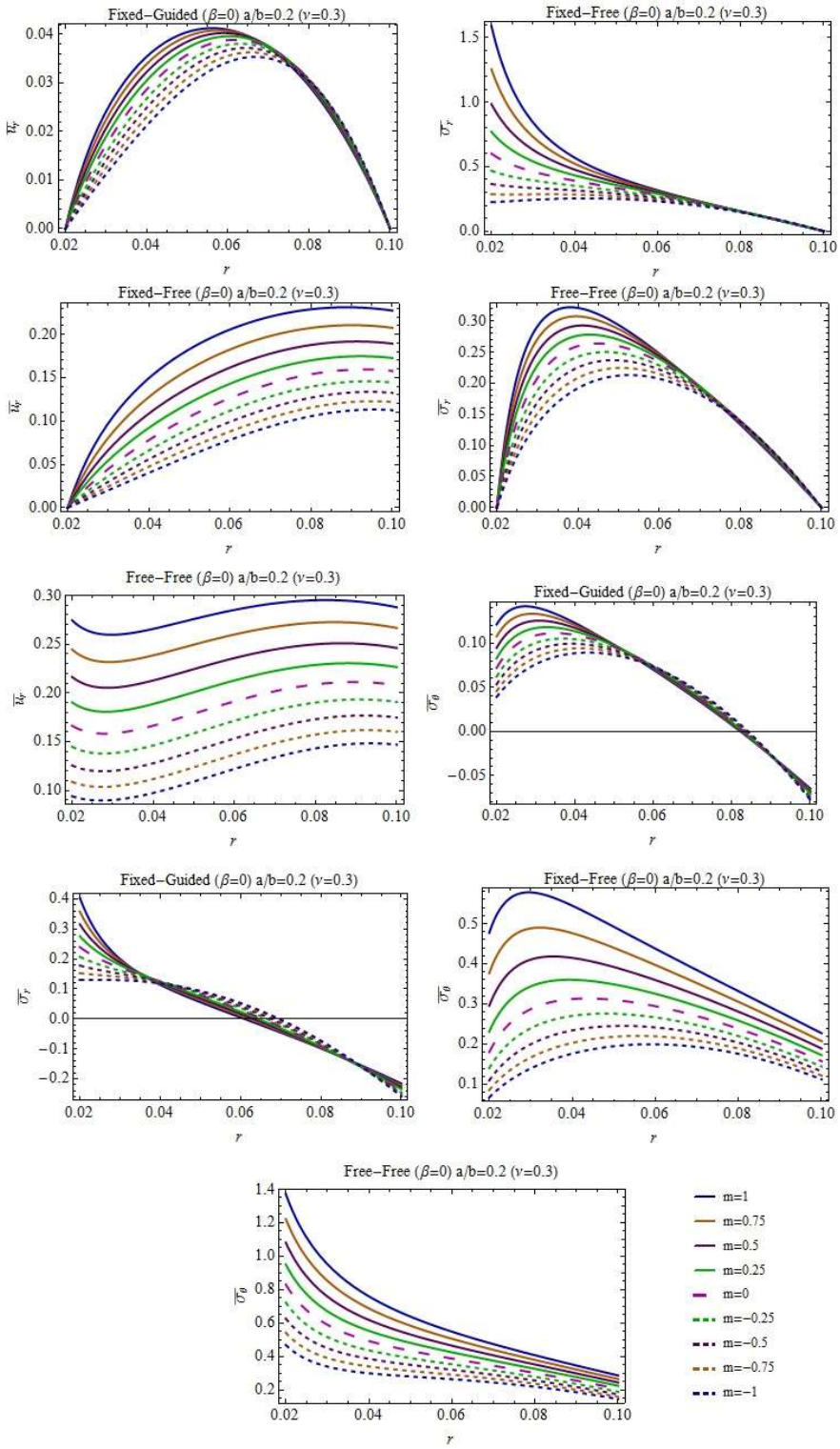

Figure 4: *Variation of the displacement, the radial and hoop stresses with the boundary conditions and profile indexes for* $\beta = 0$

Table 5: *Some numerical results for* $\beta = 0$

r/b	m=1	m=0.75	m=0.5	m=0.25	m=0	m=-0.25	m=-0.50	m=-0.75	m=-1
Dimensionless radial displacement (Free-Free)									
0.2	0.2746	0.24457	0.216397	0.19028	0.1664	0.144855	0.125665	0.108776	0.094076
0.4	0.2658	0.23860	0.212836	0.188726	0.16647	0.14618	0.127925	0.111691	0.097406
0.6	0.2852	0.26001	0.235801	0.212851	0.19136	0.171479	0.153298	0.136846	0.122101
0.8	0.2951	0.27214	0.249946	0.228775	0.20881	0.190203	0.17304	0.157363	0.143166
1.	0.2879	0.26666	0.246123	0.226513	0.208	0.190719	0.174756	0.160151	0.146899
Dimensionless radial displacement (Fixed-Free)									
0.4	0.1495	0.12772	0.108643	0.092138	0.07800	0.065996	0.055867	0.047364	0.040253
0.6	0.2057	0.18263	0.161774	0.143105	0.12654	0.111938	0.099143	0.087972	0.078246
0.8	0.2290	0.20755	0.187894	0.170079	0.15406	0.139731	0.126981	0.115666	0.105641
1.	0.2275	0.20761	0.18937	0.172807	0.15788	0.144503	0.132565	0.121942	0.1125
Dimensionless radial displacement (Fixed-Fixed)									
0.4	0.0354	0.03393	0.032276	0.030510	0.02867	0.026778	0.024887	0.023023	0.021216
0.6	0.0410	0.04072	0.040268	0.039633	0.03883	0.037868	0.036778	0.035581	0.034304
0.8	0.0295	0.02990	0.030264	0.030537	0.03071	0.03079	0.030772	0.030664	0.030474
Dimensionless radial stress (Free-Free)									
0.4	0.3212	0.30758	0.292615	0.276603	0.25988	0.24277	0.225619	0.208724	0.192345
0.6	0.2477	0.24612	0.24338	0.239538	0.23467	0.22887	0.222282	0.215051	0.207334
0.8	0.1335	0.13553	0.137187	0.138424	0.13922	0.13957	0.139489	0.139	0.138135
Dimensionless radial stress (Fixed-Free)									
0.2	1.5905	1.25541	0.985606	0.770806	0.60145	0.468979	0.36602	0.28637	0.224944
0.4	0.5702	0.52369	0.477776	0.433445	0.39144	0.352265	0.316201	0.28336	0.253716
0.6	0.3169	0.30946	0.300484	0.290295	0.27922	0.26756	0.255589	0.243534	0.231579
0.8	0.1525	0.15357	0.154053	0.153948	0.15332	0.15222	0.150731	0.148914	0.146828
Dimensionless radial stress (Fixed-Fixed)									
0.2	0.4039	0.35844	0.315752	0.276182	0.24	0.207356	0.17828	0.152691	0.130418
0.4	0.1139	0.11829	0.121622	0.123826	0.12488	0.124789	0.123635	0.121517	0.118566
0.6	0.0049	0.01104	0.017376	0.023815	0.03022	0.036466	0.042426	0.047999	0.053102
0.8	-0.098	-0.0970	-0.09511	-0.09260	-0.0895	-0.08594	-0.08190	-0.07747	-0.07274
1.	-0.216	-0.2222	-0.22845	-0.23439	-0.24	-0.24524	-0.25007	-0.2545	-0.25852
Dimensionless hoop stress (Free-Free)									
0.2	1.3728	1.22285	1.08198	0.951401	0.832	0.724276	0.628325	0.543881	0.470378
0.4	0.7608	0.68877	0.619874	0.554796	0.49413	0.43828	0.387499	0.341844	0.301219
0.6	0.5497	0.50718	0.466016	0.426613	0.38933	0.35446	0.322181	0.292592	0.265702
0.8	0.4089	0.38083	0.353588	0.327495	0.30278	0.279625	0.258146	0.238403	0.220399
1.	0.2879	0.26666	0.246123	0.226513	0.208	0.190719	0.174756	0.160151	0.146899
Dimensionless hoop stress (Fixed-Free)									
0.2	0.4771	0.37662	0.295682	0.231242	0.18043	0.140694	0.109806	0.085911	0.067483
0.4	0.5449	0.47641	0.414939	0.360378	0.31244	0.27067	0.234527	0.203418	0.176747
0.6	0.4379	0.39722	0.359768	0.325596	0.29466	0.266832	0.241915	0.219681	0.199884
0.8	0.3320	0.30551	0.281083	0.258783	0.23856	0.22033	0.203946	0.189256	0.1761
1.	0.2275	0.20761	0.18937	0.172807	0.15788	0.144503	0.132565	0.121942	0.1125
Dimensionless hoop stress (Fixed-Fixed)									
0.2	0.1212	0.10753	0.094727	0.082855	0.072	0.062207	0.053484	0.045807	0.039125
0.4	0.1228	0.12031	0.117177	0.113423	0.10913	0.104382	0.099308	0.094012	0.088610

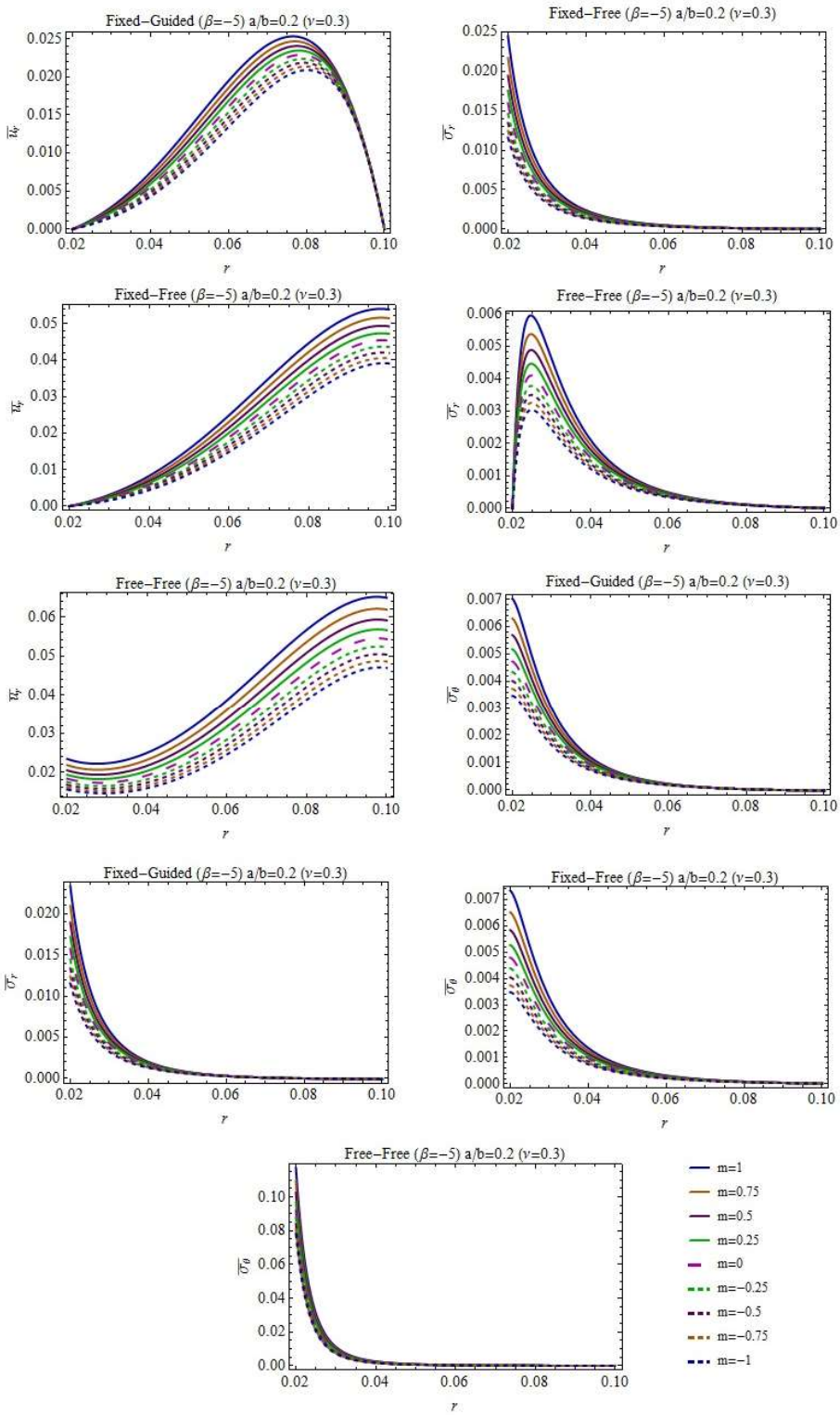

Figure 5: *Variation of the displacement, the radial and hoop stresses with the boundary conditions and profile indexes for* $\beta = -5$

Table 6: *Some numerical results for* $\beta = -5$

r/b	m=1	m=0.75	m=0.5	m=0.25	m=0	m=-0.25	m=-0.50	m=-0.75	m=-1
Dimensionless radial displacement (Free-Free)									
0.2	0.0234	0.02185	0.02051	0.01937	0.01839	0.01755	0.01682	0.016182	0.01562
0.4	0.0250	0.02320	0.02167	0.02035	0.01921	0.01822	0.01736	0.016601	0.01593
0.6	0.0386	0.03601	0.03375	0.03175	0.02997	0.02839	0.02697	0.025701	0.02456
0.8	0.0567	0.05360	0.05082	0.04830	0.04603	0.04396	0.04206	0.040333	0.03874
1	0.0649	0.06185	0.05910	0.05660	0.05433	0.05224	0.05033	0.048564	0.04693
Dimensionless radial displacement (Fixed-Free)									
0.4	0.0083	0.00754	0.00688	0.00632	0.00582	0.00539	0.00501	0.004674	0.00438
0.6	0.0249	0.02310	0.02152	0.02011	0.01884	0.01769	0.01666	0.015717	0.01486
0.8	0.0447	0.04226	0.04006	0.03805	0.03621	0.03451	0.03295	0.031499	0.03016
1	0.0538	0.05141	0.04920	0.04717	0.04529	0.04354	0.04193	0.040424	0.03902
Dimensionless radial displacement (Fixed-Fixed)									
0.4	0.0074	0.00688	0.00638	0.00593	0.00552	0.00516	0.00483	0.004536	0.00427
0.6	0.0195	0.01853	0.01765	0.01683	0.01605	0.01533	0.01465	0.014007	0.01341
0.8	0.0249	0.02438	0.02385	0.02333	0.02282	0.02231	0.02182	0.021344	0.02088
Dimensionless radial stress (Free-Free)									
0.4	0.0021	0.00195	0.00181	0.00168	0.00156	0.00146	0.00137	0.001285	0.00121
0.6	0.0005	0.00046	0.00044	0.00042	0.00040	0.00038	0.00036	0.000348	0.00033
0.8	0.0001	0.00011	0.00011	0.00010	0.00010	0.00010	0.00010	0.000095	0.00009
Dimensionless radial stress (Fixed-Free)									
0.2	0.0244	0.02171	0.01945	0.01756	0.01597	0.01463	0.01346	0.012466	0.01160
0.4	0.0024	0.00219	0.00202	0.00188	0.00175	0.00163	0.00152	0.001428	0.00134
0.6	0.0005	0.00048	0.00045	0.00043	0.00041	0.00039	0.00038	0.000359	0.00034
0.8	0.0001	0.00011	0.00011	0.00010	0.00010	0.00010	0.00010	0.000096	0.00009
Dimensionless radial stress (Fixed-Fixed)									
0.2	0.0234	0.02098	0.01895	0.01722	0.01574	0.01447	0.01336	0.012397	0.01155
0.4	0.0020	0.00190	0.00179	0.00169	0.00159	0.00151	0.00143	0.001351	0.00128
0.6	0.0003	0.00030	0.00030	0.00030	0.00029	0.00029	0.00028	0.000275	0.00027
0.8	-0.0000	-0.00001	-0.00001	-0.00000	-.000000	0.00000	0.00000	0.000007	0.00001
1.	-0.0001	-0.00009	-0.00009	-0.00009	-0.00009	-0.00009	-0.00009	-0.000092	-0.00009
Dimensionless hoop stress (Free-Free)									
0.2	0.1171	0.10924	0.10255	0.09684	0.09195	0.08774	0.08409	0.080909	0.07812
0.4	0.0026	0.00240	0.00223	0.00209	0.00197	0.00186	0.00177	0.001683	0.00161
0.6	0.0004	0.00039	0.00036	0.00034	0.00033	0.00031	0.00029	0.000281	0.00027
0.8	0.0001	0.00010	0.00009	0.00009	0.00009	0.00008	0.00008	0.000078	0.00008
1	0.0000	0.00002	0.00002	0.00002	0.00002	0.00002	0.00002	0.000016	0.00002
Dimensionless hoop stress (Fixed-Free)									
0.2	0.0073	0.00651	0.00583	0.00527	0.00479	0.00439	0.00404	0.003740	0.00348
0.4	0.0014	0.00125	0.00115	0.00106	0.00098	0.00091	0.00085	0.000794	0.00075
0.6	0.0003	0.00030	0.00028	0.00027	0.00025	0.00024	0.00023	0.000215	0.00020
0.8	0.0001	0.00008	0.00008	0.00008	0.00008	0.00007	0.00007	0.000067	0.00006
0.1	0.0000	0.00002	0.00002	0.00002	0.00001	0.00001	0.00001	0.000013	0.00001
Dimensionless hoop stress (Fixed-Fixed)									
0.2	0.0070	0.00629	0.00569	0.00517	0.00472	0.00434	0.00401	0.003719	0.00347
0.4	0.0012	0.00111	0.00104	0.00097	0.00091	0.00086	0.00081	0.000760	0.00072

4 CONCLUSIONS

After they are customized, in this study, the closed-form formulas derived by Yıldırım (2016) are employed to study the variation of the centrifugal-force-induced stress and displacements in power-law graded hyperbolic discs with inhomogeneity parameter, profile parameter, and boundary conditions. Contrary to Yıldırım's (2016) study, it is assumed that both Young's modulus and material density change with the same inhomogeneity parameter. If one suppose that *Material-a* is located at the inner surface and *Material-b* is located at the outer surface, inhomogeneity indexes should be defined by Eq. (4). Under this assumption, in practice, it is hardly confronted to get a physical metal-ceramic pair to satisfy that condition which may be defined by the following derived from Eq. (4).

$$E_a / E_b = \rho_a / \rho_b \tag{9}$$

On the other hand, in the present parametric study, Eq. (4) is not used to define the inhomogeneity indexes. Equation (3) is used by attributing hypothetically chosen values to the inhomogeneity indexes instead. For positive inhomogeneity indexes this means that while *Material-a* is located at the inner surface, the mixture of two materials which is multiples of E_a exist at the other surfaces including the outer surface. The change of the properties of the mixture is defined by Eq. (3).

Taking the same inhomogeneity index for both Young's modulus and density helps to conduct a parametric study by eliminating subordinate changes in some variables (See Eqn. (2)). That is, by doing so, we may acquire, at least, a ballpark estimate about the variation of the elastic response of hyperbolic rotating discs made of functionally graded materials. It may be noted that the formulas derived in the present study may be used for both arbitrarily chosen inhomogeneity indexes as in the parametric study and inhomogeneity indexes computed by Eq. (4).

It is obvious that analytical formulas offered by Yıldırım (2016) should be employed to get accurate results for hyperbolic discs made of physically exist material-ceramic pairs in the last decision stage of a design process.

Taking into consideration the above ball-park estimations, the true material tailoring may be done without consuming much time in the design process of such rotating hyperbolic discs made of functionally graded materials.

ACKNOWLEDGEMENTS

The author is grateful to the anonymous Referees for their valuable suggestions, the effort and time spent.

References

Apatay, T., and Eraslan, A.N. (2003). Elastic deformation of rotating parabolic discs: analytical solutions (in Turkish), Journal of the Faculty of Engineering and Architecture of Gazi University 18: 115-135.

Argeso, H. (2012). Analytical solutions to variable thickness and variable material property rotating disks for a new three-parameter variation function, Mechanics Based Design of Structures and Machines 40: 133-152.

Bayat, M., Saleem M., Sahari B., Hamouda A. and Mahdi E. (2008). Analysis of functionally graded rotating disks with variable thickness, Mechanics Research Communications 35: 283-309.

Çallıoğlu, H., Bektaþ, N.B., and Sayer, M. (2011). Stress analysis of functionally graded rotating discs: analytical and numerical solutions, Acta Mechanica Sinica 27: 950-955.

Calderale, P.M., Vivio, F., and Vullo, V. (2012). Thermal stresses of rotating hyperbolic disks as particular case of non-linearly variable thickness disks, Journal of Thermal Stresses 35: 877-891.

Eraslan, A.N. (2003a). Elastoplastic deformations of rotating parabolic solid disks using Tresca's yield criterion, European Journal of Mechanics A/Solids 22: 861–874.

Eraslan A.N. (2003b). Elastic–plastic deformations of rotating variable thickness annular disks with free, pressurized and radially constrained boundary conditions, International Journal of Mechanical Sciences 45: 643 – 667.

Eraslan, A.N., and Akış, T. (2006). On the plane strain and plane stress solutions of functionally graded rotating solid shaft and solid disk problems, Acta Mechanica 181/(1–2): 43–63.

Eraslan, A.N., and Arslan, E., (2015). Analytical and numerical solutions to a rotating FGM disk, Journal of Multidisciplinary Engineering Science and Technology (JMEST) 2/10: 2843-2850.

Eraslan, A.N., and Ciftci, B. (2015). Analytical and numerical solutions to rotating variable thickness disks for a new thickness profile, Journal of Multidisciplinary Engineering Science and Technology (JMEST) 2/9: 2359-2364.

Gang, M. (2017). Stress analysis of variable thickness rotating FG disc, International Journal of Pure and Applied Physics 13/1: 158-161.

Güven, U. (1995).Tresca's yield condition and the linear hardening rotating solid disk of variable thickness, Zeitschrift fur Angewandte Mathematik und Mechanik 75: 805 – 807.

Hassani, A., Hojjati, M.H., Farrahi, G., and Alashti, R.A. (2011). Semi-exact elastic solutions for thermomechanical analysis of functionally graded rotating disks, Composite Structures 93: 3239-3251.

Horgan, C., Chan, A. (1999a). The pressurized hollow cylinder or disk problem for functionally graded isotropic linearly elastic materials, Journal of Elasticity 55: 43-59.

Horgan, C., Chan A. (1999b). The stress response of functionally graded isotropic linearly elastic rotating disks, Journal of Elasticity 55: 219-230.

Nejad, M.Z., Abedi, M., Lotfian, M.H., and Ghannad, M. (2013) Elastic analysis of exponential FGM disks subjected to internal and external pressure, Central European Journal of Engineering 3: 459-465.

Nejad, M.Z., Rastgoo, A. and Hadi, A. (2014). Exact elasto-plastic analysis of rotating disks made of functionally graded materials, International Journal of Engineering Science 85: 47-57.

Peng, X.L., and Li, X.F. (2009). Thermoelastic analysis of a functionally graded annulus with an arbitrary gradient, Appl Math Mech. 30: 1211–1220.

Peng, X.L. and Li, X.F. (2012). Effects of gradient on stress distribution in rotating functionally graded solid disks, J. Mech. Sci. Technol. 26: 1483-1492.

Vivio, F., and Vullo, V. (2007). Elastic stress analysis of rotating converging conical disks subjected to thermal load and having variable density along the radius. International Journal of Solids and Structures 44: 7767–7784.

Vivio, F., Vullo, V., and Cifani, P. (2014). Theoretical stress analysis of rotating hyperbolic disk without singularities subjected to thermal load, Journal of Thermal Stresses, 37: 117–136.

Vullo, V., Vivio, F. (2008). Elastic stress analysis of non-linear variable thickness rotating disks subjected to thermal load and having variable density along the radius, Inter. J. Solids Struct. 45: 5337–5355.

Yıldırım, V. (2016). Analytic solutions to power-law graded hyperbolic rotating discs subjected to different boundary conditions, International Journal of Engineering & Applied Sciences (IJEAS) 8/1:38-52.

Yıldırım, V., (2017). Heat-induced, pressure-induced and centrifugal-force-induced exact axisymmetric thermo-mechanical analyses in a thick-walled spherical vessel, an infinite cylindrical vessel, and a uniform disc made of an isotropic and homogeneous material, International Journal of Engineering & Applied Sciences (IJEAS), 9 (2): 66-87.

You, L.H. You, X.Y. Zhang J.J. and Li J. (2007). On rotating circular disks with varying material properties, Z. Angew. Math. Phys., ZAMP 58: 1068–1084.

Zenkour, A.M. (2005). Analytical solutions for rotating exponentially-graded annular disks with various boundary conditions, Int. Journal of Struct. Stability and Dynamics 5: 557-577.

Zenkour, A.M. (2007). Elastic deformation of the rotating functionally graded annular disk with rigid casing, Journal of Materials Science 42: 9717-9724.

Zenkour, A.M., and Mashat, D.S. (2011). Stress function of a rotating variable-thickness annular disk using exact and numerical methods, Engineering 3: 422-430.

APPENDIX A

Under axisymmetric plane stress and small deformation assumptions, in a polar coordinate system, (r,θ), the relations between the strain and displacement components are as follows

$$\varepsilon_r(r)=\frac{d}{dr}u_r(r)$$

$$\varepsilon_\theta(r)=\frac{u_r(r)}{r} \tag{A.1}$$

Where u_r is the radial displacement; ε_r and ε_θ are the radial and tangential strain components, respectively. For an isotropic and non-homogeneous material, the stress-strain relations (Hooke's law) is

$$\sigma_r(r)=\frac{E(r)}{1-\nu^2}\left(\varepsilon_r(r)+\nu\varepsilon_\theta(r)\right)$$

$$\sigma_\theta(r)=\frac{E(r)}{1-\nu^2}\left(\varepsilon_\theta(r)+\nu\varepsilon_r(r)\right) \tag{A.2}$$

Where $E(r)$ is the elasticity modulus; ν is Poisson's ratio; σ_r and σ_θ are radial stress and circumferential stress (hoop stress), respectively. The equilibrium equation of a variable thickness disk rotating at a constant angular velocity, ω, is

$$\frac{d}{dr}\left(h(r)r\sigma_r(r)\right)-h(r)\sigma_\theta(\mathrm{r})+h(r)\rho(r)\omega^2r^2=0 \tag{A.3}$$

Where $\rho(r)$ is the material density, and $h(r)$ defines the profile of the disc, $h(r)=h_a(r/a)^m$. Substituting Eq. (A.1) in Eq. (A.2), and then Eq. (A.2) in Eq. (A.3) yields the following non-homogeneous governing equation in terms of radial displacement and its derivatives.

$$\frac{d^2}{dr^2}u_r(r)+\frac{d}{dr}u_r(r)\left(\frac{\frac{d}{dr}E(r)}{E(r)}+\frac{\frac{d}{dr}h(r)}{h(r)}+\frac{1}{r}\right)+u_r(r)\left(\frac{\nu\frac{d}{dr}E(r)}{rE(r)}-\frac{1}{r^2}+\frac{\nu\frac{d}{dr}h(r)}{rh(r)}\right)=-\frac{\omega^2r\rho(r)\left(1-\nu^2\right)}{E(r)} \tag{A.4}$$

In the above equation called Navier equation, after choosing either $E(r)=E_a(r/a)^\beta$ with $\rho(r)=\rho_a(r/a)^q$ or $E(r)=E_b(r/b)^\beta$ with $\rho(r)=\rho_b(r/b)^q$ as a material grading rule $((dE(r)/dr/E(r)=;(dh(r)/dr)/h(r)=m/r)$ then one may reach the following.

$$\frac{\left(-1+m\nu+\beta\nu\right)}{r^2}u_r(r)+\frac{\left(1+m+\beta\right)}{r}\frac{d}{dr}u_r(r)+\frac{d^2}{dr^2}u_r(r)=-\frac{r^{1+q-\beta}\left(1-\nu^2\right)\rho_a\omega^2}{E_a} \tag{A.5}$$